N-RAP scaffolds I-Z-I assembly during myofibrillogenesis in cultured chick cardiomyocytes

Stefanie Carroll, Shajia Lu, Amy H. Herrera and Robert Horowits*

Laboratory of Muscle Biology, National Institute of Arthritis and Musculoskeletal and Skin Diseases, National Institutes of Health, Department of Health and Human Services, Bethesda, MD 20892, USA

*Author for correspondence (e-mail: horowits@helix.nih.gov)

Accepted 27 August 2003
Journal of Cell Science 117, 105-114 Published by The Company of Biologists 2004
doi:10.1242/jcs.00847

Summary

N-RAP is a muscle-specific protein with an N-terminal LIM domain (LIM), C-terminal actin-binding super repeats homologous to nebulin (SR) and nebulin-related simple repeats (IB) in between the two. Based on biochemical data, immunofluorescence analysis of cultured embryonic chick cardiomyocytes and the targeting and phenotypic effects of these individual GFP-tagged regions of N-RAP, we proposed a novel model for the initiation of myofibril assembly in which N-RAP organizes α-actinin and actin into the premyofibril I-Z-I complexes. We tested the proposed model by expressing deletion mutants of N-RAP (i.e. constructs containing two of the three regions of N-RAP) in chick cardiomyocytes and observing the effects on α-actinin and actin organization into mature sarcomeres. Although individually expressing either the LIM, IB, or SR regions of N-RAP inhibited α-actinin assembly into Z-lines, expression of either the LIM-IB fusion or the IB-SR fusion permitted normal α-actinin organization. In contrast, the LIM-SR fusion (LIM-SR) inhibited α-actinin organization into Z-lines, indicating that the IB region is critical for Z-line assembly. While permitting normal Z-line assembly, LIM-IB and IB-SR decreased sarcomeric actin staining intensity; however, the effects of LIM-IB on actin assembly were significantly more severe, as estimated both by morphological assessment and by quantitative measurement of actin staining intensity. In addition, LIM-IB was consistently retained in mature Z-lines, while mature Z-lines without significant IB-SR incorporation were often observed. We conclude that the N-RAP super repeats are essential for organizing actin filaments during myofibril assembly in cultured embryonic chick cardiomyocytes, and that they also play an important role in removal of the N-RAP scaffold from the completed myofibrillar structure. This work strongly supports the N-RAP scaffolding model of premyofibril assembly.

Key words: Myofibrillogenesis, Cardiomyocytes, N-RAP, Actin

Introduction

N-RAP is a ~190 kDa actin binding LIM protein found in skeletal and cardiac muscle tissues (Luo et al., 1997; Mohiddin et al., 2003). In addition to its N-terminal LIM domain, N-RAP contains 10 or 11 simple repeats that are homologous to nebulin simple repeats, and five C-terminal nebulin-related super repeats, each composed of seven single repeats (Mohiddin et al., 2003). N-RAP is concentrated at the ends of striated muscles in adult tissues (Herrera et al., 2000; Luo et al., 1997; Zhang et al., 2001), but studies of cultured embryonic chick cardiomyocytes have implicated N-RAP in myofibril assembly (Carroll et al., 2001; Carroll and Horowits, 2000).

Many studies suggest that myofibril assembly begins at the membrane. In cultured cardiomyocytes (Dabiri et al., 1997; Rhee et al., 1994), precardiac mesoderm explant cultures (Imanaka-Yoshida et al., 1998; Rudy et al., 2001) and embryonic hearts (Ehler et al., 1999), the earliest myofibril precursors originate near the membrane. These precursors appear as immature fibrils containing punctate α-actinin Z-bodies, α-actin and muscle tropomyosin (Dabiri et al., 1997; Dlugosz et al., 1984; Handel et al., 1991; Rhee et al., 1994; Schultheiss et al., 1990; Wang et al., 1988), as well as nonmuscle myosin IIb (Rhee et al., 1994) and N-RAP (Carroll and Horowits, 2000; Lu et al., 2003). Time-lapse studies of living cardiomyocytes expressing α-actinin fused to GFP suggest that nascent myofibrils are formed by lateral aggregation of Z-bodies (Dabiri et al., 1997). The nascent myofibrils incorporate titin, and muscle myosin gradually replaces the nonmuscle isoform (Dabiri et al., 1997). Other studies suggest that bipolar muscle myosin filaments may form separately from the I-Z-I structures and that the integration of these may be controlled by interactions with titin filaments (Holtzer et al., 1997; Schultheiss et al., 1990). Titin is a giant, elongated protein that has long been thought to play a key organizational role during myofibril assembly. Periodic titin spots have been observed in the early stages of myofibrillogenesis in the chick embryo (Tokuyasu and Maher, 1987). Furthermore, in murine embryonic skeletal muscle, Z-line epitopes of titin appear to be organized earlier than regions of titin that are more centrally located within the sarcomere (Furst et al., 1989). In cultured chick cardiomyocytes, titin epitopes in the I-band and at the A/I junction become organized coincident with the appearance of periodic A-bands (Komiyama et al., 1993; Komiyama et al., 1990), but in this system the earliest I-Z-I structures formed near the cell periphery, termed premyofibrils, do not appear to contain titin (Rhee et al., 1994). However, titin was detected in the early I-Z-I structures in chick precardiac explants (Rudy et al., 2001).

Whether Z-line titin organization occurs in the very first steps of assembly or shortly thereafter, the data point to a sequence of events in which the appropriate region of titin is first incorporated into the assembling Z-disk, and other parts of the titin molecule subsequently bind to thick filaments and guide their incorporation into the periodic I-Z-I structure of the developing myofibril.

Like nonmuscle myosin IIb (Dabiri et al., 1997; Rhee et al., 1994), N-RAP is found associated with all the myofibril precursors in cultured cardiomyocytes, but is not found in the mature sarcomeres (Carroll and Horowits, 2000). This is consistent with the finding that N-RAP is absent from mature sarcomeres in cardiac and skeletal muscle from adult mice and humans (Herrera et al., 2000; Luo et al., 1997; Mohiddin et al., 2003; Zhang et al., 2001). When expressed in the cardiomyocytes as GFP fusion proteins, the individual regions of N-RAP were localized in patterns consistent with their binding activities (Lu et al., 2003; Luo et al., 1999): the talin-binding N-RAP LIM domain targeted to the cell periphery; the actin-binding super repeats (the SR region) were found in myofibril precursors and in sarcomeric actin filaments; and the α-actinin binding simple repeat region in between the LIM and SR regions (termed IB for in between) colocalized with α-actinin at the cell periphery, in myofibrillar precursors and at mature Z-lines (Carroll et al., 2001). In addition, overexpression of any of the three N-RAP regions inhibited myofibril assembly as measured by α-actinin organization into mature Z-lines, providing evidence for a functional role during assembly (Carroll et al., 2001). Based on the binding properties, targeting activities and phenotypic effects of N-RAP domains, we presented a molecular model of myofibrillogenesis initiation in which N-RAP functions as an organizing center for the sequential recruitment and assembly of α-actinin and actin (Carroll et al., 2001).

In this study, we test the proposed model by expressing deletion mutants of N-RAP in chick cardiomyocytes and observing the effects on α-actinin and actin organization into mature sarcomeres. This work provides evidence that the N-RAP IB region is essential for α-actinin organization, and that the N-RAP super repeats are essential for sarcomeric actin organization, consistent with the N-RAP scaffolding model of premyofibril assembly.

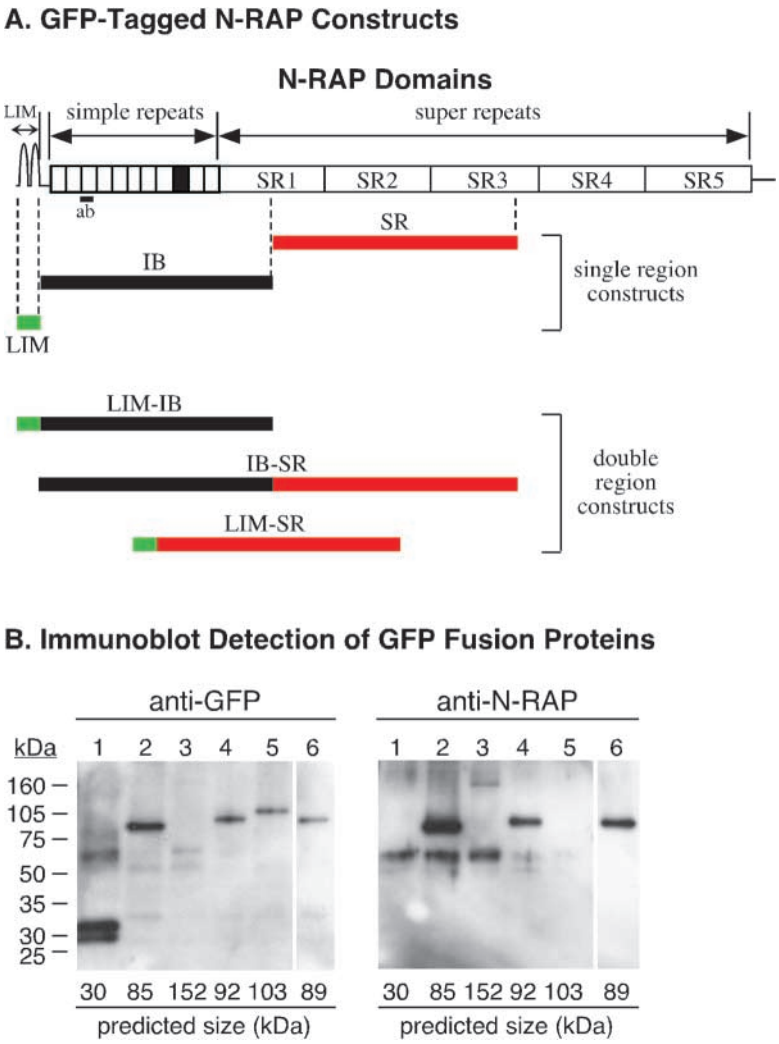

Fig. 1. (A) Schematic diagram of N-RAP domain organization (Mohiddin et al., 2003) and regions of N-RAP expressed as GFP fusion proteins. An alternatively spliced single module that is skeletal muscle-specific is shown as a filled box. The position of a 30-residue peptide used as an antigen for the production of polyclonal antibodies is marked as 'ab'. Previously described single region constructs contained GFP fused to the N terminus of the LIM, IB and SR regions. The new double region constructs contain each combination of the single regions; these include the LIM + IB construct (LIM-IB), the IB + SR construct (IB-SR) and the LIM + SR construct (LIM-SR). (B) Immunoblot analysis of chick cardiomyocytes transfected with constructs encoding GFP tagged N-RAP constructs. The cells were expressing unfused GFP (lane 1), cardiac IB (lane 2), cardiac IB-SR (lane 3), cardiac LIM-IB (lane 4), LIM-SR (lane 5) and skeletal muscle IB (lane 6). Equivalent volumes of lysate from cultured chick cardiomyocytes were loaded in each lane and probed with anti-GFP or anti-N-RAP antibodies, as indicated. In each case a band was detected migrating near the size predicted from the sequence of the fusion plasmid, which is indicated below each lane. A prominent extraneous band was sometimes also detected at ~65 kDa, but did not interfere with the identification of the intact fusion proteins.

Materials and Methods

Cloning of N-terminal GFP fusion proteins

Specific regions of the N-RAP cDNA (Fig. 1) were PCR amplified using the primer pairs described in Table 1. Cloning of the GFP-tagged LIM, IB, and SR regions has been described previously (Carroll et al., 2001). The LIM-IB region, as well as the LIM and SR regions, were PCR amplified from adult mouse skeletal muscle cDNA synthesized as previously described (Herrera et al., 2000). PCR amplification of these regions was performed using the Gibco-BRL Elongase enzyme mix (Life Technologies, Inc., Gaithersburg, MD). The amplification protocol used for the LIM-IB region and the super repeat (SR) region was 1 cycle at 94°C for 3 minutes; 45 cycles at 94°C for 30 seconds, then 59°C for 30 seconds, then 68°C for 5 minutes; and 1 cycle at 72°C for 7 minutes. The amplification protocol used for the N-RAP LIM domain was 1 cycle at 94°C for 5 minutes; 45 cycles at 94°C for 30 seconds, then 68°C for 5 minutes; and 1 cycle at 72°C for 7 minutes. The LIM-SR construct (LIM-SR) was created by digestion of the LIM and SR PCR

Table 1. PCR primer pairs

Amplified region	Primer pair	
IB	Forward: 5′-AACCCTAAGAACAACACGTTCACTAG-3′	Reverse: 5′-**CTA**CAGGGCTCTGCCCTTCATTTTC-3′
LIM-IB	Forward: 5′-ATGAATGTGCAGGCCTGCTCT-3′	Reverse: 5′-**CTA**CAGGGCTCTGCCCTTCATTTTC-3′
IB-SR	Forward: 5′-AACCCTAAGAACAACACGTTCACTAG-3′	Reverse: 5′-**CTA**CACACAGGGAACACCACGCATG-3′
LIM-SR		
LIM segment	Forward: 5′-ATGAATGTGCAGGCCTGCTCT-3′	Reverse: 5′-TGGTTAAGGTCTAGAGTGGGCGTGACAGTACGG-3′
SR segment	Forward: 5′-ACACACACATCTAGAGGAGCCACAGAC-TCTAAGCTTCTGC-3′	Reverse: 5′-**CTA**CACACAGGGAACACCACGCATG-3′

Stop codons added to each reverse primer are indicated in bold. Underlined residues mark *Xba*I endonuclease sites used to ligate the LIM and SR regions prior to cloning into the GFP-expression plasmid.

products with *Xba*I, followed by gel purification and ligation of the products prior to cloning into the GFP expression plasmid. The IB-SR region and IB region were amplified from a plasmid containing the full-length cardiac isoform of mouse N-RAP (Mohiddin et al., 2003). PCR amplification of these regions was performed using the The Advantage 2 PCR Kit (Clontech, Inc. CA). The amplification protocol was 1 cycle at 95°C for 1 minute; 35 cycles at 95°C for 30 seconds, then 68°C for 3 minutes; and 1 cycle at 68°C for 3 minutes.

PCR products were gel purified and cloned into the pcDNA3.1/NT-GFP-TOPO plasmid vector (Invitrogen Corp., Carlsbad, CA). Plasmids were propagated in One Shot TOP10 *E. coli* cells (Invitrogen, Carlsbad, CA) and purified using either the Quantum Prep Plasmid Miniprep Kit (BioRad Laboratories, Inc., Hercules, CA) or the S.N.A.P. MiniPrep Kit (Invitrogen Corp., Carlsbad, CA). Plasmids were partially sequenced to verify the integrity of the cloned inserts. In addition, the plasmids were analyzed by PCR for inclusion of the alternatively spliced exon 12 as previously described (Mohiddin et al., 2003).

Culture and transfection of chick cardiomyocytes

Primary cultures of chick cardiomyocytes were prepared from 7- to 10-day chick embryos as previously described (Carroll and Horowits, 2000) and transfected with GFP-expression constructs after 1 day in culture. The transfection mixture contained 0.5 μg of plasmid DNA and 6 μl of FuGene (Boehringer Mannheim Corp., Indianapolis, IN), a non-liposomal transfection reagent, in normal growth medium. Cultures were processed for immunoblot analysis or fluorescence microscopy as previously described (Carroll and Horowits, 2000).

For microscopy, samples were fixed 3 days after transfection and stained with monoclonal antibody against sarcomeric α-actinin (Sigma, St Louis, MO) diluted 1:2000, or monoclonal antibody against sarcomeric actin (Sigma, St Louis, MO) diluted 1:100; bound primary antibodies against α-actinin and actin were detected with rhodamine-linked secondary antibody (rabbit anti-mouse whole antibody; Sigma) diluted 1:500 or 1:100, respectively, as previously described (Carroll and Horowits, 2000).

Immunoblot analysis was performed as previously described (Carroll and Horowits, 2000). Blotted GFP fusion proteins were detected with polyclonal antibody against N-RAP (Luo et al., 1997) and monoclonal anti-GFP (Clontech Laboratories, Palo Alto, CA).

Data analysis

Cardiomyocytes were observed with a Zeiss Axiovert 135 microscope equipped for incident-light fluorescence and phase contrast microscopy using a 63× oil immersion objective with a numerical aperture of 1.25. The appropriate filters for either GFP or rhodamine fluorescence were used. Images were collected using a Photometrics CoolSnap fx CCD camera (Roper Scientific, Inc., Tucson, AZ) interfaced with a Power Macintosh computer. Quantitative image analysis was performed on a Macintosh computer using the public domain NIH Image program (developed at the US National Institutes of Health and available on the Internet at http://rsb.info.nih.gov/nih-image/).

Results

Immunoblot analysis of GFP fusion proteins

Fig. 1A illustrates the domain structure of N-RAP and the regions that were expressed as N-terminal GFP fusion proteins. We previously described expression of the individual GFP-tagged single region constructs, including the N-RAP LIM domain, the super repeat (SR) region, and the simple repeat region in between the LIM domain and the super repeats, which we term the IB region (Carroll et al., 2001). We describe expression of all three constructs that result from combining two of the three regions to form a deletion mutant: the LIM-IB region, which includes the N-terminal LIM domain and IB region but omits the super repeats, the IB-SR region, which results from combining the IB and SR regions, and the LIM-SR construct resulting from the fusion of the LIM domain and the super repeats (Fig. 1A). The LIM-IB and IB-SR regions were expressed as the cardiac isoform, which omits a single module in the IB region that is expressed only in skeletal muscle (Mohiddin et al., 2003). In addition, we expressed both cardiac and skeletal muscle isoforms of the IB construct.

Previously, we showed through immunoblot analysis that migration of the individual N-RAP regions fused to GFP was consistent with their predicted molecular masses (Carroll et al., 2001). For this study we conducted a similar analysis to confirm that the GFP-fused combined N-RAP domains were correctly expressed. As shown in Fig. 1B, immunoblot analysis detected bands of the predicted molecular masses in lysates of chick cardiomyocyte cultures expressing the GFP fusion proteins. A monoclonal antibody against GFP specifically detected bands corresponding to GFP alone, as well as the new GFP-tagged LIM-IB and LIM-SR constructs; both cardiac and skeletal isoforms of the IB construct were also detected (Fig. 1B, left panel). The same bands were detected with an antibody against N-RAP, with the exception of the LIM-SR construct, which does not contain the antigenic peptide used to create this antibody (Fig. 1B, right panel). The IB-SR construct was not efficiently detected by the antibody against GFP, but was clearly observed with the anti-N-RAP antibody, although in smaller amounts than the other constructs (Fig. 1B). The low expression level of IB-SR in transfected cultures is consistent with the inverse relation between plasmid size and transfection efficiency that we routinely observe in these cells (data not shown). A prominent extraneous band was sometimes also

detected at ~65 kDa (Fig. 1B), but did not interfere with identification of the recombinant proteins. Interestingly, a ~65 kDa band was also detected with anti-N-RAP antibodies in homogenates of adult human skeletal and cardiac muscle, but was not detected in murine muscle tissues (Mohiddin et al., 2003). The results confirm expression of the intact fusion proteins in transfected cardiomyocytes.

Effect of N-RAP deletion mutants on α-actinin organization

We expressed the new GFP-tagged N-RAP deletion mutants in cultured embryonic chick cardiomyocytes and stained the cells with antibodies against α-actinin to visualize myofibrils and myofibril precursors. As previously reported, GFP alone is diffusely distributed in transfected cells and does not interfere with myofibril assembly (Carroll et al., 2001; Mohiddin et al., 2003). Cells were transfected 1 day after plating and observed 3 days after transfection; our previous studies showed that myofibrils assemble between 2 and 4 days after plating and that these transfection conditions yield maximal inhibitory effects on myofibril assembly in response to expression of single regions of N-RAP (Carroll et al., 2001).

Fig. 2 shows cells expressing the LIM-SR construct, which contains the N-RAP LIM domain fused to two super repeats. This construct was sometimes expressed in a diffuse pattern (Fig. 2A), but was most often observed along the cell periphery and along fibers continuously stained for α-actinin (Fig. 2D). The variable localization patterns observed for LIM-SR were unrelated to its expression level, as estimated from the average pixel intensity of GFP fluorescence determined from the raw images. LIM-SR appeared to have a significant effect on the α-actinin organization, preventing Z-line organization which was lower than in neighboring untransfected cells (Fig. 2).

In contrast, the LIM-IB construct, which contains the N-RAP LIM domain and IB region but not the super repeats, co-localized with α-actinin at the cell periphery, in myofibril precursors and at mature Z-lines (Fig. 3). No disruption of the α-actinin organization was observed with this construct.

The targeting patterns of the IB-SR construct, which lacks the N-RAP LIM domain, were similar to LIM-IB, including colocalization with α-actinin at Z-lines (Fig. 4). However, this finding was less consistent and some areas filled with mature Z-lines seemed to exclude IB-SR, even though IB-SR was associated with Z-lines elsewhere in the same cell (Fig. 4D-F). In addition, in many cases IB-SR targeting in mature myofibrils appeared to extend into the I-band, suggesting incorporation into the sarcomeric actin filaments (Fig. 4A-C insets).

We quantitated Z-disk accumulation in cultured cardiomyocytes using a morphometric method illustrated in Fig. 3 (Carroll et al., 2001). GFP fluorescence in transfected cardiomyocytes was used to mark the boundaries of the cells (Fig. 3A), and α-actinin organization into broad periodic bands was used to define mature Z-disks (Fig. 3B). The ratio of total mature Z-disk-containing areas to the total cell area yields a reproducible measure of this aspect of myofibril assembly (Carroll et al., 2001). The effects of N-RAP constructs on Z-disk content is summarized in Fig. 5. The single region N-RAP

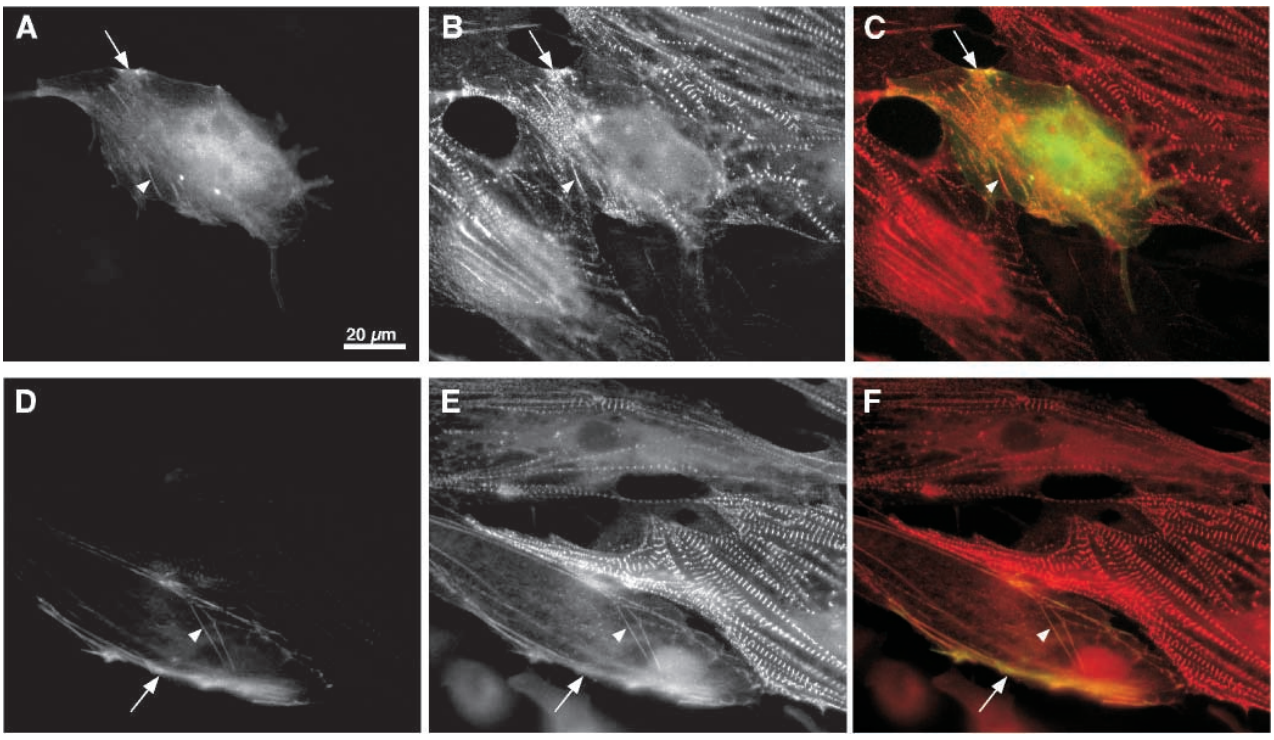

Fig. 2. Expression patterns of GFP-tagged LIM-SR (A,D), α-actinin in the same fields (B,E), and the merged images with LIM-SR and α-actinin in the green and red channels, respectively (C, F). In some cells LIM-SR is diffusely distributed (A), but it is most often concentrated at the cell periphery (arrows) and along fibers continuously stained for α-actinin (arrowheads). The transfected cells in A and D exhibit LIM-SR expression levels that do not differ by more than a factor of two when normalized to cell area. LIM-SR expression appears to have disrupted α-actinin organization into periodic striations when compared with neighboring untransfected cells.

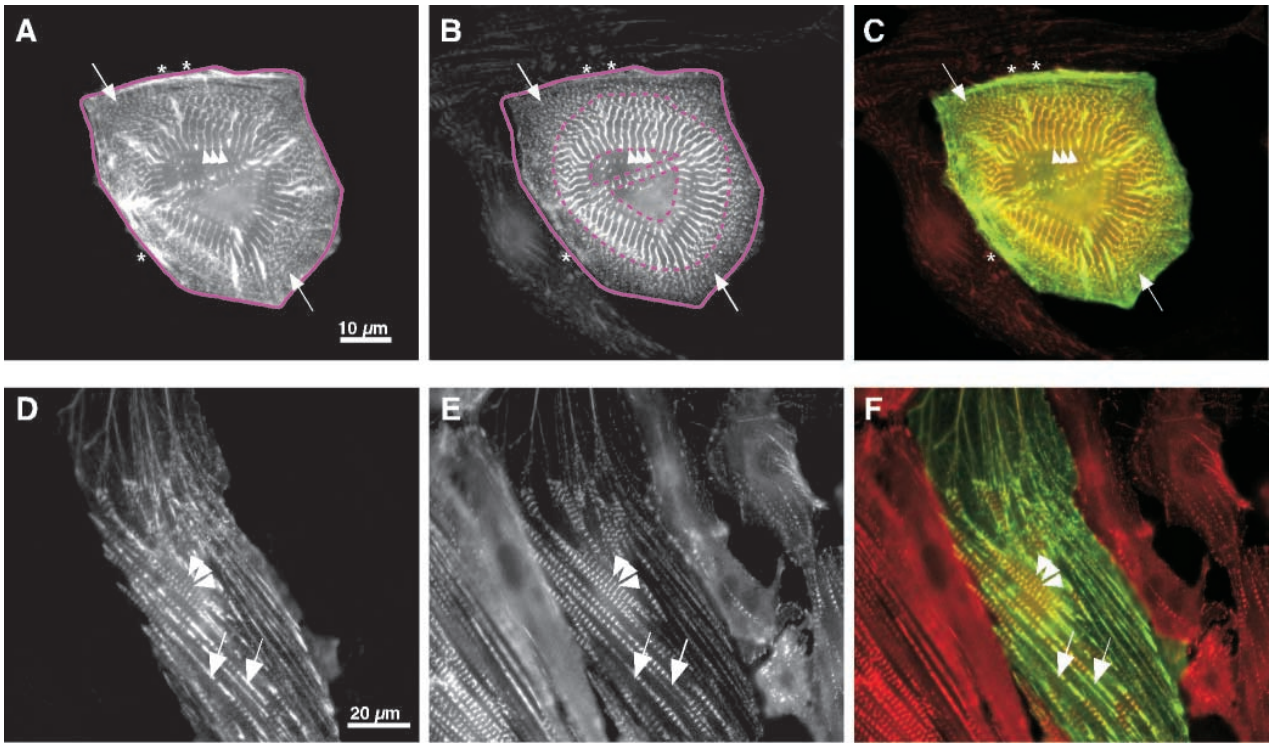

Fig. 3. Expression patterns of GFP-tagged LIM-IB (A,D), α-actinin in the same fields (B,E) and the merged images with LIM-IB and α-actinin in the green and red channels, respectively (C,F). LIM-IB was co-localized with α-actinin at the cell periphery (asterisks), in myofibril precursors (arrows), and at Z-lines (arrowheads), with no apparent disruption of α-actinin organization. Summing the striated areas visualized by α-actinin staining (areas within dashed magenta lines in B) and dividing by the total cell area visualized by GFP fluorescence (area within the solid magenta line in A) yields a morphometric measure of myofibril content (Carroll et al., 2001).

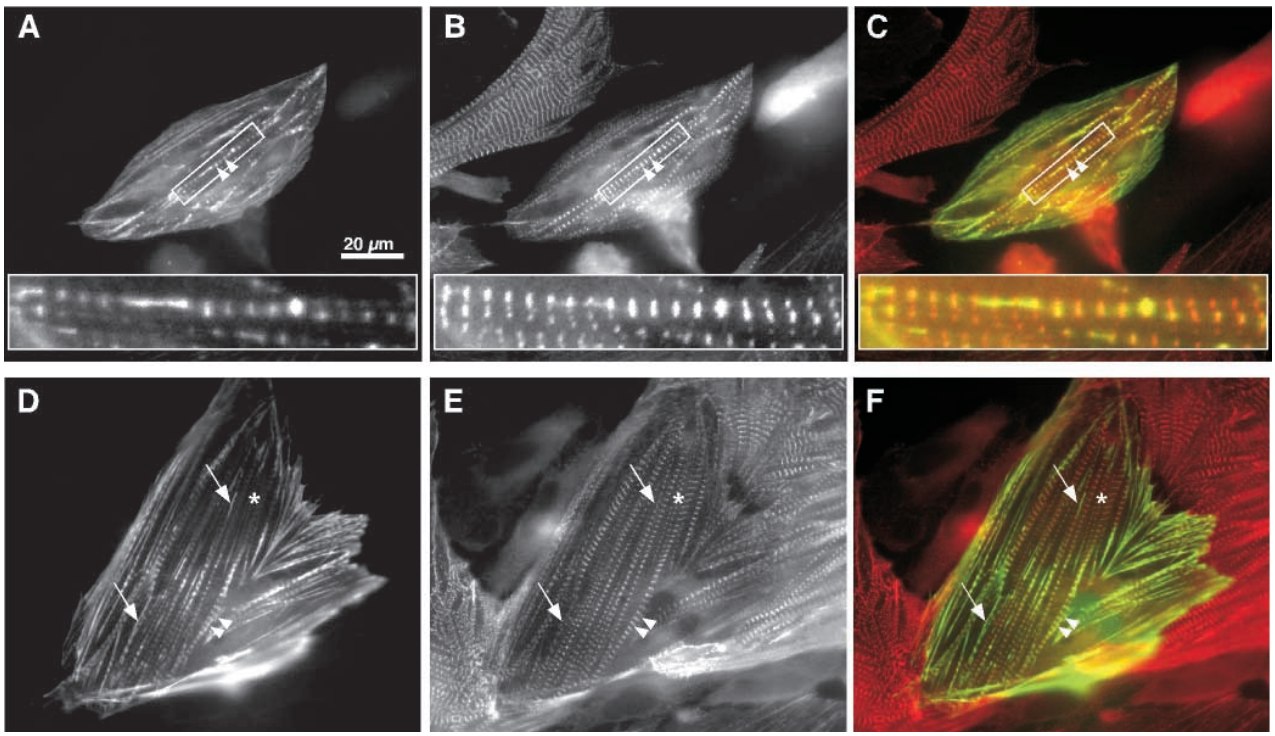

Fig. 4. Expression patterns of GFP-tagged IB-SR (A,D), α-actinin in the same fields (B,E), and the merged images with IB-SR and α-actinin in the green and red channels, respectively (C,F). In many areas IB-SR was co-localized with α-actinin at Z-lines (arrowheads), but in some areas IB-SR appeared to be excluded from mature Z-lines (D-F, asterisk). IB-SR fluorescence often extended beyond the Z-lines, marking the entire I-bands (A-C, inset). In addition, IB-SR fluorescence appeared continuous in immature regions where myofibrils appeared to be fusing laterally (arrows).

constructs inhibited Z-disk assembly compared to GFP alone, as previously reported. We found that both cardiac and skeletal muscle forms of the IB region are equally effective in inhibiting Z-disk assembly (Fig. 5). Of the deletion mutants, only LIM-SR significantly inhibited α-actinin assembly into Z-lines, while LIM-IB and IB-SR did not have significantly reduced Z-disk content, as measured by α-actinin assembly (Fig. 5). None of the constructs significantly altered total α-actinin levels as measured by the mean pixel intensity of α-actinin staining (data not shown).

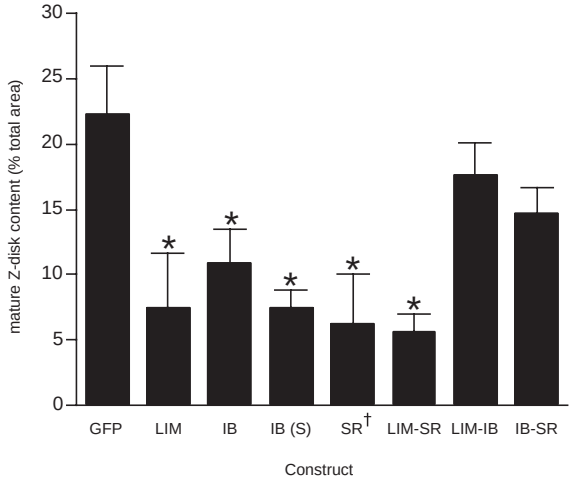

Fig. 5. Effect of GFP-tagged N-RAP constructs on Z-disk content as indicated by morphometric measurements of α-actinin organization into broad striations. Results for both cardiac and skeletal muscle (S) isoforms of the IB construct are shown; LIM-IB and IB-SR, the other two constructs containing the IB region, are both cardiac isoforms. Each bar represents the mean ± s.e.m. of 12-53 transfected cells. *Significant difference from GFP alone (P<0.05); †previously published data (Carroll et al., 2001).

Effect of N-RAP deletion mutants on actin organization

Since we hypothesize that N-RAP domains organize α-actinin and actin assembly in the first steps of myofibrillogenesis, actin assembly may be affected in cases where α-actinin assembly into Z-lines is normal. Therefore, we observed actin organization in cardiomyocytes transfected with the LIM-IB and IB-SR constructs, which do not significantly affect α-actinin organization relative to cardiomyocytes expressing unfused GFP.

Fig. 6 shows examples of cardiomyocytes expressing the IB-SR construct and stained with an antibody against sarcomeric actin. In some cases, IB-SR appeared to be concentrated in a narrow band at the Z-line (Fig. 6, top row), while in other cells we observed broad bands of IB-SR localization coinciding with the sarcomeric actin filaments in the I-bands (Fig. 6, bottom row). The actin organization appeared normal with either localization pattern of IB-SR, with broad bands of actin similar to those observed in untransfected cells (compare Fig. 6B and 6E with Fig. 7D).

In contrast, incorporation of the LIM-IB construct into myofibrillar Z-lines was often associated with disrupted actin organization. Fig. 7 shows a transfected cardiomyocyte in which LIM-IB is localized in mature Z-lines. Within this cell, there are regions in which the actin associated with LIM-IB-

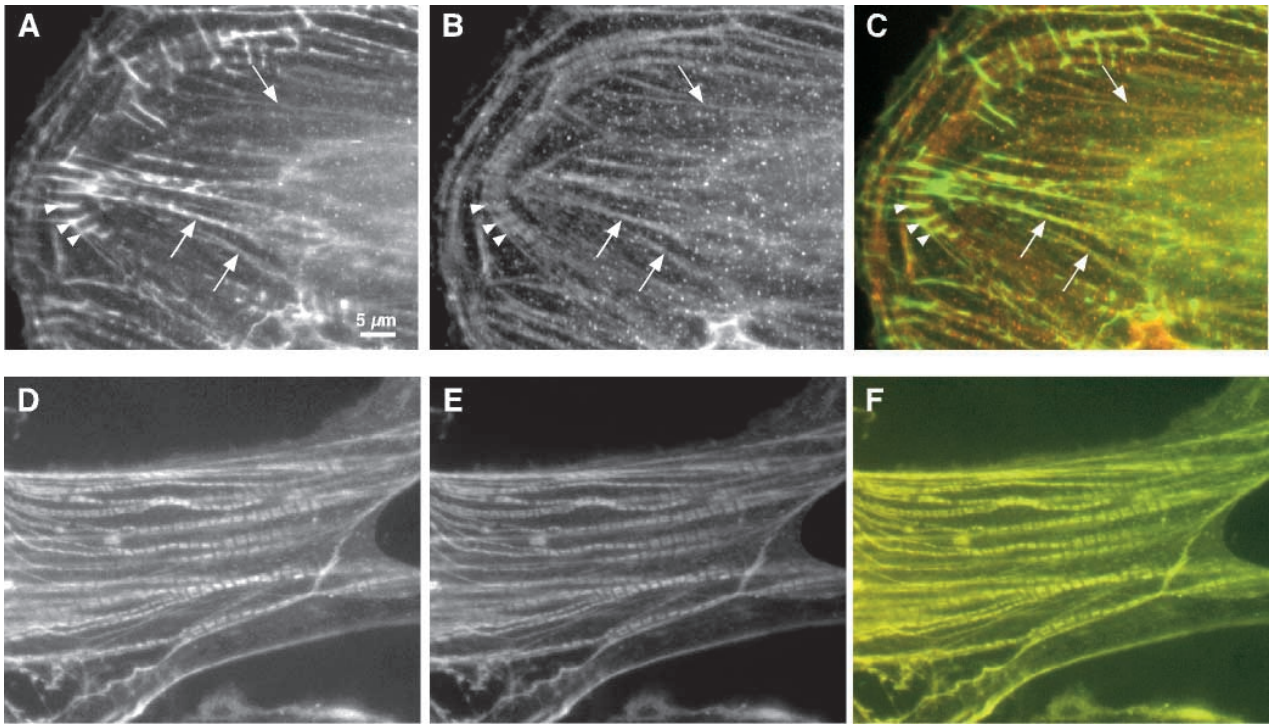

Fig. 6. Expression patterns of GFP-tagged IB-SR (A,D), actin in the same fields (B,E), and the merged images with IB-SR and actin in the green and red channels, respectively (C,F). In some cases IB-SR was localized in narrow bands at apparent Z-lines associated with broad-banded actin staining in the I-bands (A-C, arrowheads). In other cases IB-SR colocalized with actin in the I-bands (D-F). In addition, IB-SR colocalized with actin in nonstriated fibers (arrows).

containing Z-lines is less organized than in untransfected controls (Fig. 7B, arrowheads), as well as regions in which there is no detectable actin associated with well defined Z-lines marked by LIM-IB fluorescence (Fig. 7B, arrow). The gross morphological observations suggest that LIM-IB incorporation into Z-lines leads to disrupted actin organization within the sarcomere, while IB-SR incorporation into Z-lines or actin filaments does not interfere with the normal assembly of actin and α-actinin into I-Z-I structures.

Within some cells there appeared to be an inverse correlation between LIM-IB fluorescence at the Z-line and actin organization in the same sarcomeres. Fig. 8A shows a cardiomyocyte in which there is an apparent gradient of LIM-IB incorporation into myofibrillar Z-lines. Sarcomeres with less LIM-IB fluorescence at the Z-lines appear to have normal actin staining (Fig. 8A-C, arrowheads), but actin is disorganized or absent in sarcomeres with more intense LIM-IB fluorescence at the Z-lines (Fig. 8A-C, asterisk). We quantitated the GFP fluorescence intensity at the Z-line, along with the actin staining intensity in the associated I-bands (Fig. 8D). In many cells there was an inverse relation between the two (Fig. 8E), indicating that LIM-IB incorporation results in disruption of sarcomeric actin assembly.

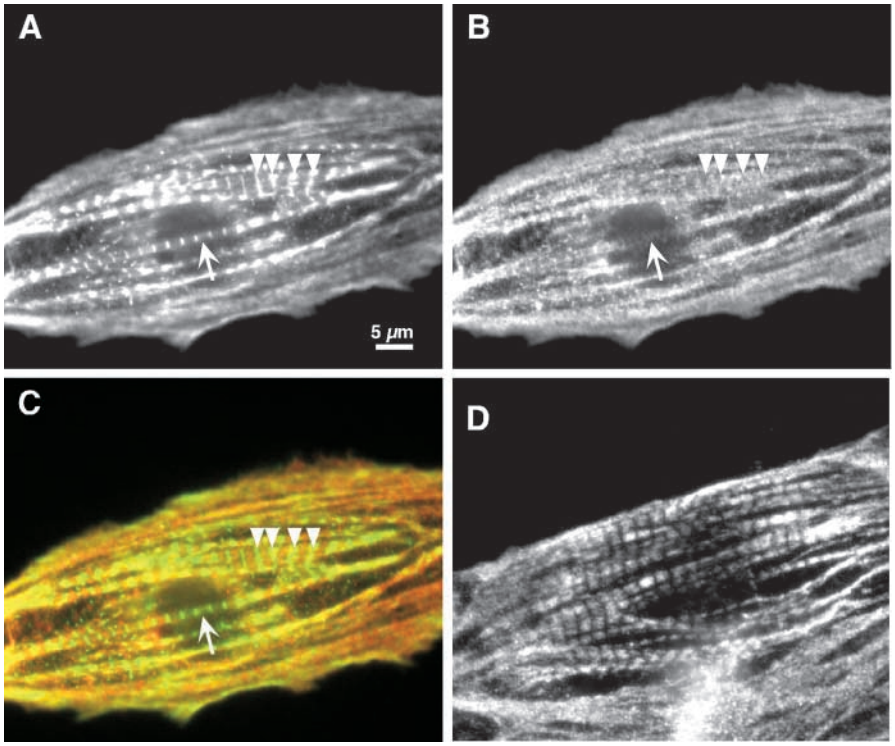

Fig. 7. Expression patterns of GFP-tagged LIM-IB (A), actin in the same fields (B), and the merged images with LIM-IB and actin in the green and red channels, respectively (C). Actin staining in an untransfected cell is shown for comparison (D). LIM-IB was consistently found in appropriately spaced Z-lines (arrowheads). Actin in normal sarcomeres is organized into well-defined broad bands (D), but in sarcomeres incorporating LIM-IB at the Z-line, actin staining is more amorphous or severely reduced (arrowheads and arrow, respectively).

The effects of LIM-IB and IB-SR constructs on actin organization are summarized in Table 2. Both LIM-IB and IB-SR expression resulted in decreased intensity of sarcomeric actin staining compared to untransfected controls, even though morphological disruption of actin assembly was only observed in the LIM-IB-transfected cells. However, actin staining intensity was more severely affected by LIM-IB expression ($P<0.05$). Sarcomere length was unaffected by these constructs (Table 2).

Table 2. Actin assembly

Construct	Actin assembly (relative units)	Sarcomere length (μm)
Untransfected	1.00±0.06	1.67±0.02
LIM-IB	0.40±0.03	1.62±0.02
IB-SR	0.62±0.06	1.61±0.04

Actin staining in sarcomeres was measured as illustrated in Fig. 8. Each value is the mean±s.e.m. of 39-238 measurements. Analysis of variance indicates all actin assembly values are significantly different from each other ($P<0.05$); sarcomere lengths are not significantly different between groups.

Discussion

Targeting of N-RAP domains

We found that the targeting of the double N-RAP constructs was equivalent to the sum of the two regions present in the molecule. Like the IB region alone (Carroll et al., 2001), the N-RAP LIM-IB and IB-SR constructs colocalized with α-actinin at the cell periphery, in myofibril precursors and in Z-lines; in addition, the IB-SR construct was found in myofibrillar I-bands, presumably because of the binding affinity of the SR region for actin (Luo et al., 1999). LIM-SR was generally concentrated at the cell periphery and in nonstriated fibers. In general, the targeting is consistent with the IB region binding α-actinin, the SR region binding actin and the LIM domain targeting to complexes at the membrane (Carroll et al., 2001; Luo et al., 1999).

Disruption of myofibrillogenesis by N-RAP deletion mutants

The embryonic chick cardiomyocyte culture system yields a mixture of cells that vary greatly with respect to cell shape, extent of spreading and myofibril accumulation. While the micrographs presented show typical examples of transfected cells, conclusions regarding the effects of recombinant proteins on myofibril assembly can only be made based on quantitative analysis of the transfected cells. The morphometric analysis of striated α-actinin provides a reproducible measure of Z-line assembly (Carroll et al., 2001), while actin staining intensity provides a measure of sarcomeric actin assembly. Together, these quantitative assays allow us to examine the effects of recombinant proteins on assembly of the major structural components of the I-Z-I complex.

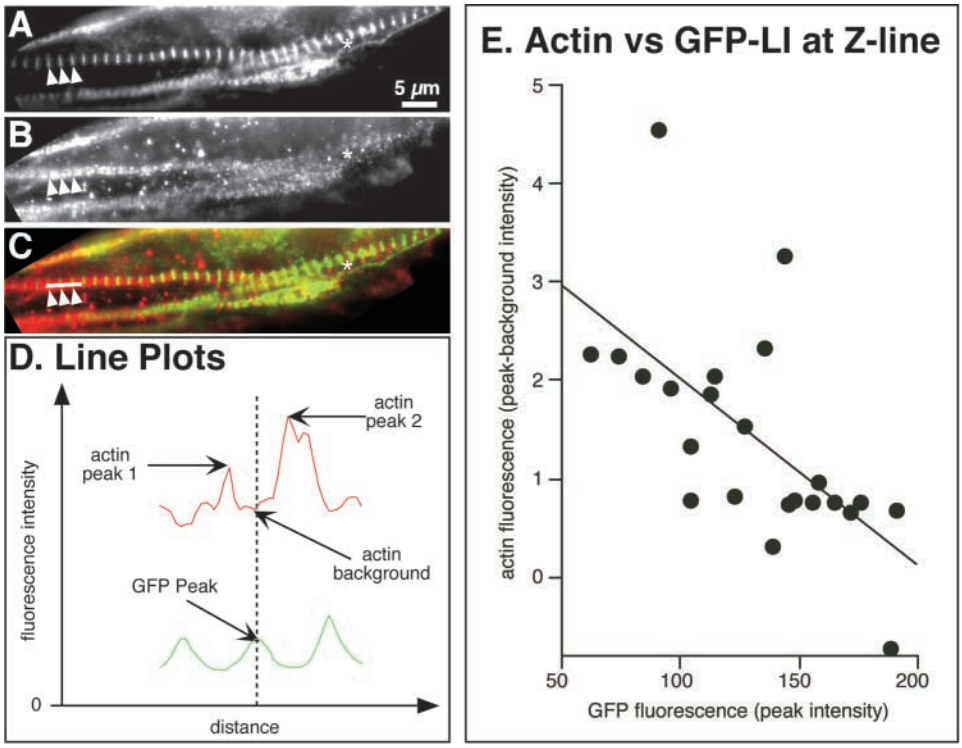

Fig. 8. (A-C) A cardiomyocyte with sarcomeres containing varying amounts of GFP-tagged LIM-IB at the Z-lines. (A) GFP-LIM-IB fluorescence appears to increase from left to right in this field. (B) Actin staining is strong in the sarcomeres at the left side of the field (arrowheads), but decreases as GFP fluorescence increases (asterisk). (C) The merged LIM-IB fluorescence and actin staining are shown in the green and red channels, respectively. (D) Line plots along the long axis of the myofibril were used to quantitate fluorescence intensity of GFP incorporation and actin staining. Plots from the region marked by a white line in C are shown in D. The peak GFP intensity at the Z-line was measured, and the actin peaks in the associated half sarcomeres around the Z-line were measured along with the actin background staining intensity. The specific actin staining was taken as the difference between the peak and background levels. (E) Specific actin staining intensity is plotted versus the peak GFP-LIM-IB fluorescence at the Z-line for sarcomeres in the cell in A-C. There is a significant negative correlation between LIM-IB incorporation at the Z-line and actin content in the associated half sarcomeres (P<0.05).

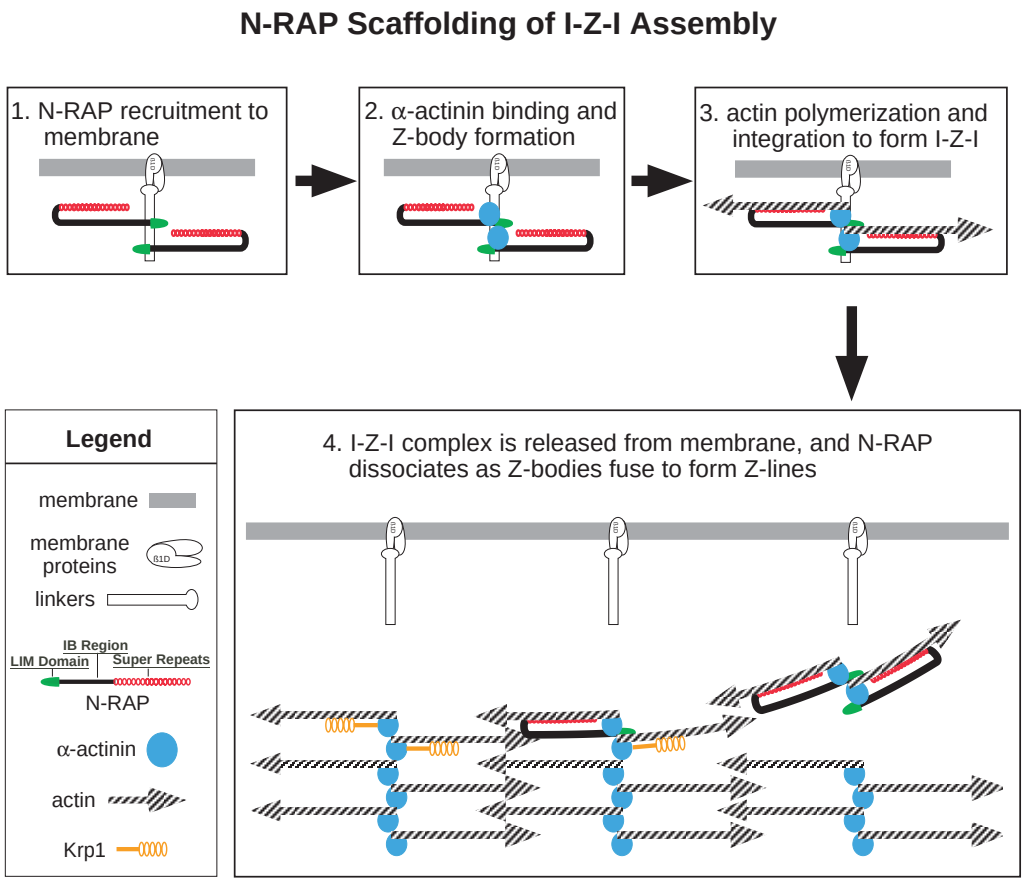

Fig. 9. Schematic model illustrating N-RAP scaffolding during assembly of the I-Z-I complex. (1) N-RAP binds to a membrane-associated complex containing integral membrane and linker components. (2) α-actinin is recruited to the complex. (3) Actin polymerizes along the N-RAP super repeats, with the barbed end of the actin filament integrating with α-actinin at the Z-body. The orientation of the actin filament is indicated by an arrowhead at the pointed end. (4) The premyofibril I-Z-I complex is released from the membrane, and N-RAP dissociates as the Z-bodies fuse laterally to form mature Z-lines. Krp1 is hypothesized to play a role in N-RAP dissociation from the nascent myofibril.

Our previous studies showed that the embryonic chick cardiomyocytes round up and disassemble any preexisting contractile structures after dissociation and plating (Carroll and Horowits, 2000). Between 2 and 4 days after plating, the cells assemble striated myofibrils (Carroll et al., 2001). Therefore, we interpreted a lack of myofibrils after transfection with plasmids encoding N-RAP constructs as an inhibition of myofibril assembly. Overexpression of the N-RAP LIM domain, the IB region, or the super repeats severely disrupted myofibril assembly (Carroll et al., 2001). Our current studies show that deletion mutants containing two of these three regions exhibit targeting effects consistent with the targeting of individual domains, but affect myofibril assembly in a manner consistent with a stepwise mechanism in which N-RAP functions as a molecular scaffold to organize α-actinin and actin into I-Z-I structures. The results clearly show that overexpression of the LIM-IB construct permits normal organization of α-actinin into Z-lines, while LIM-SR does not permit Z-line assembly. However, LIM-IB does disrupt actin organization and in some cells this disruption is quantitatively related to LIM-IB incorporation at the Z-line. The results indicate that the α-actinin binding IB region is essential for Z-line assembly, while the actin binding SR region is essential for sarcomeric actin assembly.

Like LIM-IB, the IB-SR construct also allowed normal α-actinin assembly, but its effects on actin assembly were significantly less severe, as estimated both by morphological assessment and by quantitative measurement of actin staining intensity. In addition, LIM-IB was consistently retained in mature Z-lines, while mature Z-lines without significant IB-SR incorporation were often observed. We conclude that the SR region plays an important role in removal of the N-RAP scaffold from the completed myofibrillar structure.

N-RAP scaffolding of I-Z-I assembly

Fig. 9 illustrates a scheme for N-RAP scaffolding of I-Z-I assembly that is consistent with the binding and targeting activities of the different regions of N-RAP, as well with the effects of each of these regions on myofibril assembly when expressed singly or as fused constructs in cultured cardiomyocytes. The first step involves binding of N-RAP to a membrane-associated complex that may include both integral membrane proteins and linker molecules. Oppositely oriented N-RAP molecules are hypothesized as a way of establishing the mirror image symmetry of the I-Z-I complex. In the second step, α-actinin is recruited to the complex, and this is followed by actin polymerization promoted by the N-RAP super repeats in the third step. The concept of actin organization by N-RAP super repeats is consistent with the promotion of actin polymerization by nebulin repeats in vitro (Chen et al., 1993; Gonsior et al., 1998), as well as with the linear organization of nebulin in sarcomeric actin filaments (Herrera et al., 2000; Wang et al., 1996; Wright et al., 1993); these considerations suggest that the N-RAP scaffold controls the polarity of newly formed actin filaments in the I-Z-I complex and provides a means of integrating the barbed ends with the α-actinin at the Z-bodies. In the fourth step the newly formed I-Z-I complex is released from its membrane attachments and fuses laterally with other developing myofibrillar structures to form the mature Z-lines with their associated actin filaments. N-RAP exits the complex during this stage. Krp1 (also called sarcosin) is a muscle-specific kelch-repeat protein (Spence et al., 2000; Taylor et al., 1998) that localizes near laterally fusing myofibrils but does not appear to be organized earlier in the assembly process (Lu et al., 2003). Since Krp1 binds the N-RAP super repeats and the IB region (Lu et al., 2003) and has repeating motifs that are putative actin binding sites (Spence et al., 2000; Taylor et al., 1998), we hypothesize that Krp1 is involved in catalyzing the lateral fusion of Z-bodies and the removal of N-RAP from the complex.

This work provides evidence that the N-RAP IB region is essential for α-actinin organization, and that the N-RAP super repeats are essential for sarcomeric actin organization and for removal of N-RAP from the complex. Although this work was performed using recombinant mouse N-RAP fragments in chick cardiomyocytes, it appears that the N-RAP protein (Mohiddin et al., 2003) and key features of myofibril assembly (Sanger et al., 2002) are well conserved among vertebrate species. Important general questions that remain to be answered include the identity of the integral membrane proteins and linker molecules that tether the I-Z-I complex to the membrane, how the initial periodicity of the Z-bodies near the membrane is determined, and how the Z-body spacing is increased during maturation. In addition, the role of nonmuscle myosin IIb in the premyofibril (Dabiri et al., 1997; Rhee et al., 1994), the mechanism of early assembly of other Z-line components such as filamin (Bechtel, 1979; Koteliansky et al., 1985; Lu et al., 2003; Mittal et al., 1987; Price et al., 1994; Thompson et al., 2000; van der Ven et al., 2000a; van der Ven et al., 2000b) and nebulette (Moncman and Wang, 1995; Moncman and Wang, 1999) and the mechanism by which the I-Z-I complex is integrated with bipolar muscle myosin filaments (Holtzer et al., 1997; Schultheiss et al., 1990) are questions that must be answered for a thorough understanding of myofibril assembly at the molecular level.

References

Bechtel, P. J. (1979). Identification of a high molecular weight actin-binding protein in skeletal muscle. *J. Biol. Chem.* **254**, 1755-1758.

Carroll, S. L., Herrera, A. H. and Horowits, R. (2001). Targeting and functional role of N-RAP, a nebulin-related LIM protein, during myofibril assembly in cultured chick cardiomyocytes. *J. Cell Sci.* **114**, 4229-4238.

Carroll, S. L. and Horowits, R. (2000). Myofibrillogenesis and formation of cell contacts mediate the localization of N-RAP in cultured chick cardiomyocytes. *Cell Motil. Cytoskeleton* **47**, 63-76.

Chen, M. J., Shih, C. L. and Wang, K. (1993). Nebulin as an actin zipper. A two-module nebulin fragment promotes actin nucleation and stabilizes actin filaments. *J. Biol. Chem.* **268**, 20327-20334.

Dabiri, G. A., Turnacioglu, K. K., Sanger, J. M. and Sanger, J. W. (1997). Myofibrillogenesis visualized in living embryonic cardiomyocytes. *Proc. Natl. Acad. Sci. USA* **94**, 9493-9498.

Dlugosz, A. A., Antin, P. B., Nachmias, V. T. and Holtzer, H. (1984). The relationship between stress fiber-like structures and nascent myofibrils in cultured cardiac myocytes. *J. Cell Biol.* **99**, 2268-2278.

Ehler, E., Rothen, B. M., Hämmerle, S. P., Komiyama, M. and Perriard, J.-C. (1999). Myofibrillogenesis in the developing chicken heart: assembly of the z-disk, m-line and thick filaments. *J. Cell Sci.* **112**, 1529-1539.

Furst, D. O., Osborn, M. and Weber, K. (1989). Myogenesis in the mouse embryo: differential onset of expression of myogenic proteins and the involvement of titin in myofibril assembly. *J. Cell Biol.* **109**, 517-527.

Gonsior, S. M., Gautel, M. and Hinssen, H. (1998). A six-module human nebulin fragment bundles actin filaments and induces actin polymerization. *J. Muscle Res. Cell. Motil.* **19**, 225-235.

Handel, S. E., Greaser, M. L., Schultz, E., Wang, S. M., Bulinski, J. C.,

Lin, J. J. and Lessard, J. L. (1991). Chicken cardiac myofibrillogenesis studied with antibodies specific for titin and the muscle and nonmuscle isoforms of actin and tropomyosin. *Cell Tissue Res.* **263**, 419-430.

Herrera, A. H., Elzey, B., Law, D. J. and Horowits, R. (2000). Terminal regions of mouse nebulin: sequence analysis and complementary localization with N-RAP. *Cell Motil. Cytoskeleton* **45**, 211-222.

Holtzer, H., Hijikata, T., Lin, Z. X., Zhang, Z. Q., Holtzer, S., Protasi, F., Franzini-Armstrong, C. and Sweeney, H. L. (1997). Independent assembly of 1.6 microns long bipolar MHC filaments and I-Z- I bodies. *Cell Struct. Funct.* **22**, 83-93.

Imanaka-Yoshida, K., Knudsen, K. A. and Linask, K. K. (1998). N-cadherin is required for the differentiation and initial myofibrillogenesis of chick cardiomyocytes. *Cell Motil. Cytoskeleton* **39**, 52-62.

Komiyama, M., Maruyama, K. and Shimada, Y. (1990). Assembly of connectin (titin) in relation to myosin and alpha-actinin in cultured cardiac myocytes. *J. Muscle. Res. Cell Motil.* **11**, 419-428.

Komiyama, M., Kouchi, K., Maruyama, K. and Shimada, Y. (1993). Dynamics of actin and assembly of connectin (titin) during myofibrillogenesis in embryonic chick cardiac muscle cells in vitro. *Dev. Dyn.* **196**, 291-299.

Koteliansky, V. E., Shirinsky, V. P., Gneushev, G. N. and Chernousov, M. A. (1985). The role of actin-binding proteins vinculin, filamin, and fibronectin in intracellular and intercellular linkages in cardiac muscle. *Adv. Myocardiol.* **5**, 215-221.

Lu, S., Carroll, S. L., Herrera, A. H., Ozanne, B. and Horowits, R. (2003). New N-RAP-binding partners α-actinin, filamin and Krp1 detected by yeast two-hybrid screening: implications for myofibril assembly. *J. Cell Sci.* **116**, 2169-2178.

Luo, G., Zhang, J. Q., Nguyen, T. P., Herrera, A. H., Paterson, B. and Horowits, R. (1997). Complete cDNA sequence and tissue localization of N-RAP, a novel nebulin-related protein of striated muscle. *Cell Motil. Cytoskeleton* **38**, 75-90.

Luo, G., Herrera, A. H. and Horowits, R. (1999). Molecular interactions of N-RAP, a nebulin-related protein of striated muscle myotendon junctions and intercalated disks. *Biochemistry* **38**, 6135-6143.

Mittal, B., Sanger, J. M. and Sanger, J. W. (1987). Binding and distribution of fluorescently labeled filamin in permeabilized and living cells. *Cell Motil. Cytoskeleton* **8**, 345-359.

Mohiddin, S. A., Lu, S., Cardoso, J.-P., Carroll, S. L., Jha, S., Horowits, R. and Fananapazir, L. (2003). Genomic organization, alternative splicing, and expression of human and mouse N-RAP, a nebulin-related LIM protein of striated muscle. *Cell Motil. Cytoskeleton* **55**, 200-212.

Moncman, C. L. and Wang, K. (1995). Nebulette: a 107 kD nebulin-like protein in cardiac muscle. *Cell Motil. Cytoskeleton* **32**, 205-225.

Moncman, C. L. and Wang, K. (1999). Functional dissection of nebulette demonstrates actin binding of nebulin-like repeats and Z-line targeting of SH3 and linker domains. *Cell Motil. Cytoskeleton* **44**, 1-22.

Price, M. G., Caprette, D. R. and Gomer, R. H. (1994). Different temporal patterns of expression result in the same type, amount, and distribution of filamin (ABP) in cardiac and skeletal myofibrils. *Cell Motil. Cytoskeleton* **27**, 248-261.

Rhee, D., Sanger, J. M. and Sanger, J. W. (1994). The premyofibril: evidence for its role in myofibrillogenesis. *Cell Motil. Cytoskeleton* **28**, 1-24.

Rudy, D. E., Yatskievych, T. A., Antin, P. B. and Gregorio, C. C. (2001). Assembly of thick, thin, and titin filaments in chick precardiac explants. *Dev. Dyn.* **221**, 61-71.

Sanger, J. W., Chowrashi, P., Shaner, N. C., Spalthoff, S., Wang, J., Freeman, N. L. and Sanger, J. M. (2002). Myofibrillogenesis in skeletal muscle cells. *Clin. Orthop. Relat. Res.* S153-162.

Schultheiss, T., Lin, Z. X., Lu, M. H., Murray, J., Fischman, D. A., Weber, K., Masaki, T., Imamura, M. and Holtzer, H. (1990). Differential distribution of subsets of myofibrillar proteins in cardiac nonstriated and striated myofibrils. *J. Cell Biol.* **110**, 1159-1172.

Spence, H. J., Johnston, I., Ewart, K., Buchanan, S. J., Fitzgerald, U. and Ozanne, B. W. (2000). Krp1, a novel kelch related protein that is involved in pseudopod elongation in transformed cells. *Oncogene* **19**, 1266-1276.

Taylor, A., Obholz, K., Linden, G., Sadiev, S., Klaus, S. and Carlson, K. D. (1998). DNA sequence and muscle-specific expression of human sarcosin transcripts. *Mol. Cell Biochem.* **183**, 105-112.

Thompson, T. G., Chan, Y. M., Hack, A. A., Brosius, M., Rajala, M., Lidov, H. G., McNally, E. M., Watkins, S. and Kunkel, L. M. (2000). Filamin 2 (FLN2): A muscle-specific sarcoglycan interacting protein. *J. Cell Biol.* **148**, 115-126.

Tokuyasu, K. T. and Maher, P. A. (1987). Immunocytochemical studies of cardiac myofibrillogenesis in early chick embryos. II. Generation of alpha-actinin dots within titin spots at the time of the first myofibril formation. *J. Cell Biol.* **105**, 2795-2801.

van der Ven, P. F., Obermann, W. M., Lemke, B., Gautel, M., Weber, K. and Furst, D. O. (2000a). Characterization of muscle filamin isoforms suggests a possible role of gamma-filamin/ABP-L in sarcomeric Z-disc formation. *Cell Motil. Cytoskeleton* **45**, 149-162.

van der Ven, P. F., Wiesner, S., Salmikangas, P., Auerbach, D., Himmel, M., Kempa, S., Hayess, K., Pacholsky, D., Taivainen, A., Schroder, R. et al. (2000b). Indications for a novel muscular dystrophy pathway. gamma-filamin, the muscle-specific filamin isoform, interacts with myotilin. *J. Cell Biol.* **151**, 235-248.

Wang, K., Knipfer, M., Huang, Q. Q., van Heerden, A., Hsu, L. C., Gutierrez, G., Quian, X. L. and Stedman, H. (1996). Human skeletal muscle nebulin sequence encodes a blueprint for thin filament architecture: sequence motifs and affinity profiles of tandem repeats and terminal SH3. *J. Biol. Chem.* **271**, 4304-4314.

Wang, S. M., Greaser, M. L., Schultz, E., Bulinski, J. C., Lin, J. J. and Lessard, J. L. (1988). Studies on cardiac myofibrillogenesis with antibodies to titin, actin, tropomyosin, and myosin. *J. Cell Biol.* **107**, 1075-1083.

Wright, J., Huang, Q. Q. and Wang, K. (1993). Nebulin is a full-length template of actin filaments in the skeletal muscle sarcomere: an immunoelectron microscopic study of its orientation and span with site-specific monoclonal antibodies. *J. Muscle Res. Cell Motil.* **14**, 476-483.

Zhang, J. Q., Elzey, B., Williams, G., Lu, S., Law, D. J. and Horowits, R. (2001). Ultrastructural and biochemical localization of N-RAP at the interface between myofibrils and intercalated disks in the mouse heart. *Biochemistry* **40**, 14898-14906.